

PSFC/JA-04-6

Study of Laser Plasma Interactions Using an Eulerian Vlasov Code

D. J. Strozzi, M. M. Shoucri*,
and A. Bers

March 2004

Plasma Science and Fusion Center
Massachusetts Institute of Technology
Cambridge, MA 02139 U.S.A.

* Institut de Recherche de l'Hydro Québec
Varenes, Québec, J3X 1S1, Canada

This work was supported by the U.S. Department of Energy, Grant No. DE-FG02-91ER-54109. Reproduction, translation, publication, use and disposal, in whole or in part, by or for the United States government is permitted.

To appear in *Computer Physics Communications*.

Study of laser plasma interactions using an Eulerian Vlasov code

D. J. Strozzi ^{a,*}, M. M. Shoucri ^b, A. Bers ^a

^a*Plasma Science and Fusion Center, Massachusetts Institute of Technology, Cambridge, MA*

^b*Institut de Recherche de l'Hydro Québec, Varennes, Canada*

Abstract

We present a one-dimensional Eulerian Vlasov code for performing kinetic simulations of laser-plasma interactions. We use the code to study parametric instabilities, in particular stimulated Raman scattering. For conditions similar to those of single-hot-spot experiments, we find that kinetic effects are important in the saturation of this instability. Work is underway to make the code to 1 $\frac{1}{2}$ and 2D (resolving y and p_y) and parallelize it.

Key words: Laser-plasma interaction, Eulerian Vlasov code

PACS: 52.65.Ff, 52.35.Mw, 52.38.Bv

1 Introduction

Laser-plasma interactions are an important concern for indirect-drive inertial confinement fusion. The relevant physical regimes, such as those for the National Ignition Facility, allow for the excitation of parametric instabilities, for example Stimulated Raman Scattering (SRS) and Stimulated Brillouin Scattering (SBS) [1]. We present studies of parametric instabilities using a one-dimensional Eulerian Vlasov code. The code solves the relativistic Vlasov equation for both species in the direction of laser propagation, and includes a cold-fluid velocity parallel to the laser electric field. We investigate numerically conditions similar to the recent Trident single-hot-spot experiments [2]. We are particularly concerned with the growth and saturation of SRS. The

* Corresponding author.

Email address: dstrozzi@mit.edu (D. J. Strozzi).

coupling to Langmuir Decay Instability (LDI) and detuning due to electron trapping have both been proposed as SRS saturation mechanisms [3]. For the present Trident-motivated parameters, we do not observe LDI of the SRS electron plasma wave when the SRS signal is strongest. Instead, the electron distribution shows large vortices and a beam. This suggests SRS has saturated due to kinetic effects and not LDI.

2 The Model Equations

We allow spatial variation of fields along the laser wavenumber $\vec{k}_0 = k_0 \hat{x}$ and assume uniformity in y and z . The plasma is finite in x with no imposed periodicity. Instead, we imagine two “absorbing plates” transparent to the laser at the boundaries $x = 0$ and $x = L$. As particles leave the domain $0 < x < L$, they are collected on the plates and no longer evolve (there is no reflection of particles). The accumulated charge contributes locally to E_x and leads to a sheath on both boundaries.

We restrict electric and magnetic field components to $\vec{E} = (E_x, E_y, 0)$ and $\vec{B} = (0, 0, B_z)$. E_x is the longitudinal electrostatic field and is calculated from Poisson’s equation $\partial_x E_x = \epsilon_0^{-1} \rho$. The only charge present is that on the left and right “plates” Q_l and Q_r , and the charge in the plasma Q_p from $x = 0$ to $x = L$. The field due to a uniformly-charged plate gives the boundary condition on E_x :

$$E_x(x = 0) = \frac{1}{2\epsilon_0}(Q_l - Q_p - Q_r) \quad (1)$$

If $Q_l + Q_p + Q_r = 0$, Eq. (1) is equivalent to $E_x(x = 0) = \epsilon_0^{-1} Q_l$.

E_y and B_z arise from the laser and plasma currents. We impose a laser incident from the left ($x \leq 0$) as an electromagnetic wave (k_x, E_y, B_z) . We represent the transverse fields via $E^\pm = E_y \pm cB_z$. From the Maxwell equations we find an advection equation for these fields

$$(\partial_t \pm c\partial_x)E^\pm = -\epsilon_0^{-1} J_y \quad (2)$$

E^+ and E^- represent right- and left-moving fields, respectively. In these variables, the laser in free space is given by $E^+ = E_0 \sin(k_0 x - \omega_0 t)$, $E^- = 0$. We apply the laser by setting $E^+(x = 0) = E_0 \sin \omega_0 t$, and assume there is no reflection at the right boundary ($E^-(x = L) = 0$). The advection equation then propagates E^+ in from the left and for $n_e \ll n_{cr} \equiv \epsilon_0 m_e \omega_0^2 / e^2$ gives no noticeable reflection when the laser reaches the right boundary. This allows for runs much longer than the time it takes the laser to cross the plasma.

Each species is represented by a distribution function $F_s(x, p_x, P_y, t) = \delta(P_y)f_s(x, p_x, t)$ where $P_y = m_s v_{ys} + q_s A_y$ is the canonical y momentum. Such an F_s with a cold beam in y is an exact solution of the Vlasov equation. f_s is governed by the one-dimensional relativistic Vlasov equation:

$$\frac{\partial f_s}{\partial t} + v_s \frac{\partial f_s}{\partial x} + q_s (E_x + v_{ys} B_z) \frac{\partial f_s}{\partial p_x} = 0 \quad (3)$$

The cold-fluid y momentum equation for $v_{ys}(x, t)$ reduces to conservation of P_y :

$$m_s \frac{\partial v_{ys}}{\partial t} = q_s E_y \quad (4)$$

3 Numerical Methods

We use a one-dimensional Eulerian Vlasov code based on the algorithm described in [4]. The code advances f_s from time t to $t + dt$ using the method of fractional steps with cubic spline interpolation. The forces are applied at the intermediate time $t + dt/2$ in a “leapfrog” scheme, based on the electromagnetic fields at this time. (We modify the leapfrog algorithm by combining the two free-streaming steps for f_s in order to save runtime, which gives equivalent results up to the algorithm’s order of accuracy.) We “split” the time-stepping operator into free-streaming in x and acceleration in p_x . We first advect f_s from t to $t + dt^-$ via the force-free Vlasov equation

$$\partial_t f_s + v_s \partial_x f_s = 0 \quad (5)$$

We calculate the new charge density $\rho(t + dt)$, and use the average $\rho(t + dt/2)$ in Poisson’s equation to calculate $E_x(t + dt/2)$. We then advect E^\pm with $J_y = 0$ from time t to $t + dt^-$. This allows us to advance v_{ys} by dt using an average E^\pm at $t + dt/2$. We then apply $J_y(t + dt)$ as a delta-function “kick” to take E^\pm from $t + dt^-$ to $t + dt^+$. Finally, we find the approximate force at $t + dt/2$ to advect f_s from $t + dt^-$ to $t + dt$ in momentum-space via

$$\partial_t f_s + q_s (E_x + v_{ys} B_z) \partial_{p_x} f_s = 0 \quad (6)$$

We determine the charge on the left plate at $x = 0$ by finding the number of particles that flow to the left plate in the timestep dt : $\Delta N_{sl} = -dt \int_{-\infty}^0 v_x f_s(x = 0, p_x) dp_x$ (and similarly on the right). Although the number of particles in each species should be conserved, we do not explicitly enforce this.

4 Studies of Parametric Instabilities

Parametric instabilities occur strongly when three natural modes of a plasma with frequencies ω_i and wavenumbers k_i ($i = 1, 2, 3$) satisfy the matching conditions (in one dimension) $\omega_1 = \omega_2 + \omega_3$, $k_1 = k_2 + k_3$. SRS involves a pump (here, the laser) and daughter electromagnetic wave (EMW) and a daughter electron plasma wave (EPW), while SBS involves a pump and daughter EMW, and a daughter ion acoustic wave (IAW). A large-amplitude EPW can be the pump for the Langmuir Decay Instability (LDI), which involves a daughter EPW and a daughter IAW.

We study physical regimes similar to the Trident single-hot-spot experiments. A laser with free-space wavelength $\lambda_0 = 527$ nm and intensity 10^{16} W/cm² shines on an electron-proton plasma of length $L = 73$ μ m. The plasma is initially Maxwellian with $T_e = 350$ eV, $T_i = 100$ eV, $n_e = n_i = 0.032n_{cr}$, and is homogeneous in space (except for ramping down to zero density near the boundaries).

Once the laser enters a region of the plasma, it produces small-amplitude oscillations. SRS grows from these fluctuations; we do not impose a perturbation to “seed” it. This is in contrast to earlier work, where an initial density or current perturbation, or a secondary, left-propagating laser at the SRS frequency, were added excite SRS.

Figure 1 shows the instantaneous reflectivity and power spectra of $E^-(\omega)$ at $x = 0$. The backscattered E^- grows until it reaches a maximum near $\omega_p t = 400$. Almost all the power at this time is in the SRS EMW. In the later spectrum, however, the “SRS” peak is upshifted compared to the value predicted by matching. Some power also appears at the SBS EMW frequency. We performed a run with identical parameters except that the ions were fixed ($f_i(t) = f_i(t = 0)$). The reflectivity and power spectra were basically the same, except that there is no SBS peak at late times. This shows that LDI or any other ion dynamics do not stop the growth of the first SRS peak for these parameters.

Figure 2 displays the power spectrum of $E_x(k)$ at $\omega_p t = 400$ (a) and $\omega_p t = 850$ (b). Fig. 2a shows prominently the SRS EPW peak. The peaks at $2k_{EPW}$ and $3k_{EPW}$ seem to be harmonics of the SRS EPW. Although peak at $2k_{EPW} \approx 20\omega_p/c$ is near k_{IAW} for the first Langmuir decay of the SRS EPW, it is not LDI since it also appears in the run with fixed ions. The $E_x(k)$ spectrum at $\omega_p t = 850$ in Fig. 2b is mostly broadband. The narrow line at $k\omega_p/c \approx 1$ may be related to forward Raman scattering, which is observed in the transmitted E^+ signal at the right wall $x = L$ (both the Stokes and anti-Stokes lines are present).

The contour plot of f_e at $\omega_p t = 400$ shown in Fig. 3a reveals substantial vortices and trapping centered at the phase velocity of the SRS EPW. The spatially-averaged f_e consists of a beam for $p > 0$ and bump due to trapping, superimposed on a drifting Maxwellian. We note that the amplitude of E_x at this time is above the threshold for wave-breaking [6], and that the electron temperature increases significantly once SRS develops. However, Fig. 3 shows the distribution to be highly non-Maxwellian, and “temperature” ($= n^{-1} \int (v - \langle v \rangle)^2 f dv$) should be understood in this light. The interaction of a laser with such a beam, and with a trapped distribution, may give rise to new phenomena, including the recently-observed stimulated electron acoustic scattering [5]. We are currently investigating this possibility.

The authors acknowledge fruitful conversations with Dr. A. K. Ram. The work at MIT was supported by DoE Contract DE-FG02-91ER-54109.

References

- [1] J. Lindl, *Phys. Plasmas*, **2** (1995) 3933.
- [2] D. S. Montgomery, J. A. Cobble, et al., *Phys. Plasmas*, **9** (2002) 2311.
- [3] H. X. Vu, D. F. DuBois, and B. Bezzerides, *Phys. Rev. Lett.*, **86** (2001) 4306.
- [4] A. Ghizzo, P. Bertrand, M. Shoucri, et al., *J. Comp. Phys.*, **90** (1990) 431.
- [5] A. Salcedo, R. J. Focia, A. K. Ram, and A. Bers, *Proc. 19th Fusion Energy Conference*, Lyon, France, October 2002; accepted for publication in *Nuclear Fusion*.
- [6] T. P. Coffey, *Phys. Fluids*, **14** (1971) 1402.

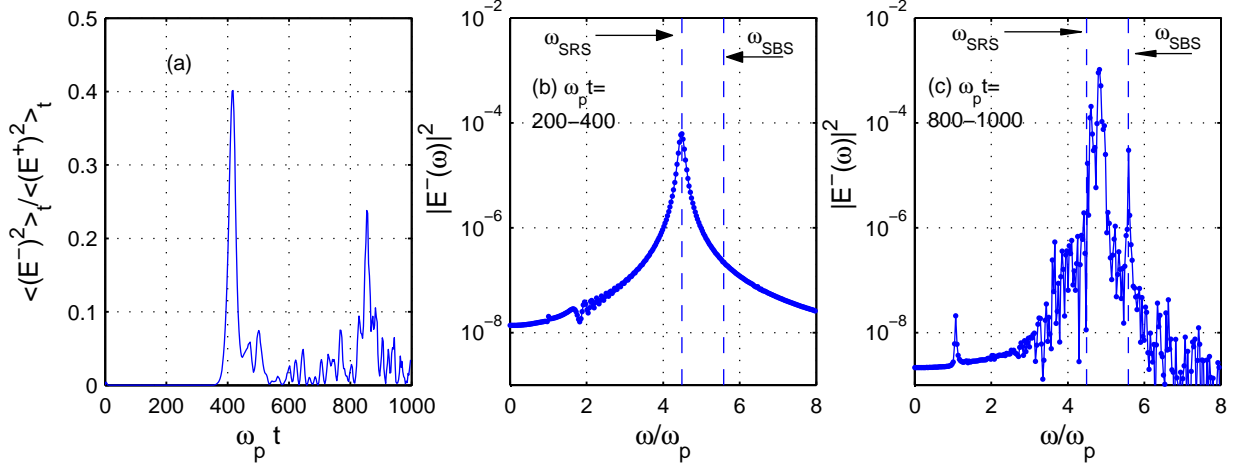


Fig. 1. (a) SRS Reflectivity at the left boundary. Power spectrum of $E^-(\omega)$ from (b) $\omega_p t = 200$ to 400 and (c) $\omega_p t = 800$ to 1000. The vertical lines are the EMW frequency from matching for SRS ($\omega_{SRS} = 4.49\omega_p$) and SBS ($\omega_{SBS} = 5.58\omega_p \approx \omega_{las} = 5.59\omega_p$).

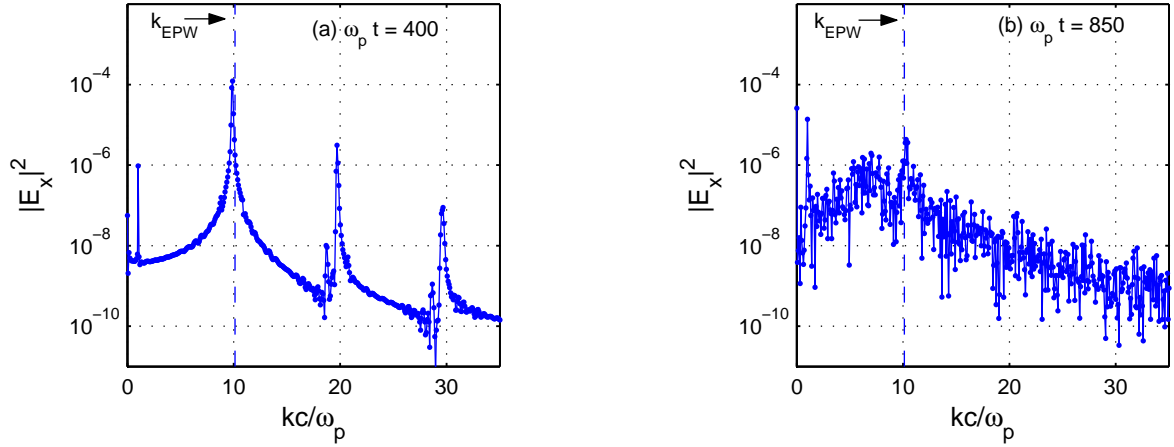


Fig. 2. Power spectrum of $E_x(k)$ from $x\omega_p/c = 20$ to 100 at $\omega_p t = 400, 850$ for (a),(b) respectively. The vertical lines are at the k 's from matching for the SRS EPW and the IAW in the first LDI cascade of the SRS EPW.

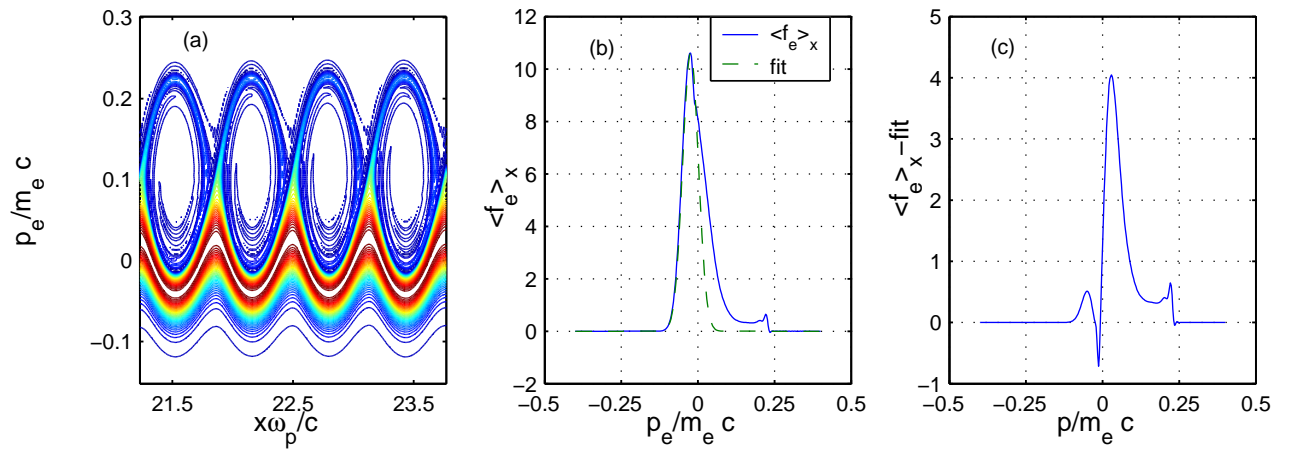


Fig. 3. (a) Contour plot of f_e at $\omega_p t = 400$. (b) Spatially-averaged f_e over the region shown in a. The dashed curve is a maxwellian fitted to points to the left of the peak of the averaged f_e . (c) Averaged f_e minus the fitted maxwellian.